2019

TARGETED ILLUMINATION STRATEGIES FOR HYDROGEN PRODUCTION FROM PURPLE NON-SULFUR BACTERIA

John D. Craven
University of Kentucky, johndcraven@gmail.com
Author ORCID Identifier:
https://orcid.org/0000-0001-5057-7703
Digital Object Identifier: https://doi.org/10.13023/etd.2019.332

STUDENT AGREEMENT:

I represent that my thesis or dissertation and abstract are my original work. Proper attribution has been given to all outside sources. I understand that I am solely responsible for obtaining any needed copyright permissions. I have obtained needed written permission statement(s) from the owner(s) of each third-party copyrighted matter to be included in my work, allowing electronic distribution (if such use is not permitted by the fair use doctrine) which will be submitted to UKnowledge as Additional File.

I hereby grant to The University of Kentucky and its agents the irrevocable, non-exclusive, and royalty-free license to archive and make accessible my work in whole or in part in all forms of media, now or hereafter known. I agree that the document mentioned above may be made available immediately for worldwide access unless an embargo applies.

I retain all other ownership rights to the copyright of my work. I also retain the right to use in future works (such as articles or books) all or part of my work. I understand that I am free to register the copyright to my work.

REVIEW, APPROVAL AND ACCEPTANCE

The document mentioned above has been reviewed and accepted by the student's advisor, on behalf of the advisory committee, and by the Director of Graduate Studies (DGS), on behalf of the program; we verify that this is the final, approved version of the student's thesis including all changes required by the advisory committee. The undersigned agree to abide by the statements above.

John D. Craven, Student

Dr. Dibakar Bhattacharyya, Major Professor

Dr. Stephen Rankin, Director of Graduate Studies

TARGETED ILLUMINATION STRATEGIES FOR HYDROGEN PRODUCTION FROM PURPLE NON-SULFUR BACTERIA

THESIS

A thesis submitted in partial fulfillment of the
requirements for the degree of Master of Science in Chemical Engineering
in the College of Engineering
at the University of Kentucky

By

John David Craven

Lexington, Kentucky

Director: Dr. Dibakar Bhattacharyya, Professor of Chemical Engineering

Lexington, Kentucky

2019

https://orcid.org/0000-0001-5057-7703

ABSTRACT OF THESIS

TARGETED ILLUMINATION STRATEGIES FOR
HYDROGEN PRODUCTION FROM PURPLE NON-SULFUR BACTERIA

The movement towards a more sustainable energy economy may require not only the generation of cleaner fuel sources, but the conversion of waste streams into value-added products. Phototrophic purple non-sulfur bacteria are capable of metabolizing VFAs (volatile fatty acids)and generate hydrogen as a byproduct of nitrogen fixation using energy absorbed from light. VFAs are easily produced from dark anaerobic fermentation of food, agricultural, and municipal wastes, which could then be fed into photobioreactors of purple bacteria for hydrogen production.

The process of photofermentation by purple bacteria for hydrogen production remains attractive due to the capability of reaching high substrate conversions under mild operating conditions, but increasing the efficiency of converting light energy into hydrogen remains challenging. Purple bacteria cannot utilize the entire solar spectrum, and the dominant region of absorption lies in the near-infrared region above 800 nm.

In this work, the model purple non-sulfur bacteria *Rhodopseudomonas palustris* was used to study different strategies to increase light utilization and hydrogen production. Near-infrared LED arrays were selected to match the target bacteriochlorophyll absorption range, and were tested to be used as a sole illumination source for photofermentation. Additionally, plasmonic nanoparticles with resonant frequencies matching bacterial absorbance were added in solution to increase light utilization through scattering and near field electric enhancement effects at intensities around 100 W/m^2. Both of these approaches proved to increase cellular growth rate and hydrogen production, which opens the door to utilizing more advanced photonic structures for use in bacterial phototrophic processes.

KEYWORDS: photofermentation, purple non-sulfur bacteria, hydrogen, near-infrared, plasmonic nanoparticles

John David Craven
(Name of Student)

07/18/2019
Date

TARGETED ILLUMINATION STRATEGIES FOR HYDROGEN PRODUCTION FROM PURPLE NON-SULFUR BACTERIA

By
John David Craven

Dibakar Bhattacharyya
Director of Thesis

Stephen Rankin
Director of Graduate Studies

07/18/2019
Date

ACKNOWLEDGMENTS

The following thesis benefited from the insights and encouragement provided by my Thesis Chair Dr. Dibakar Bhatacharyya, who has pushed me to become a better researcher. I would like to thank Dr. Todd Hastings, Dr. Doo Young Kim, and Dr. Sarah Wilson for helping to guide my research. I would also like to thank Rupam Sarma for his help in conducting experiments and contributing to CO_2 analysis. I would also like to thank Mansoor Sultan for his contributions to nanoparticle characterization, and light measurement techniques. Finally I would like to thank the members of the Bhattacharyya research group, who provided support throughout my research.

This work could not have been completed without support provided by National Science Foundation EAGER Grant 1700091, NSF EPSCoR grant 1355438, and Southern Company.

TABLE OF CONTENTS

LIST OF TABLES

LIST OF FIGURES

CHAPTER 1. INTRODUCTION AND BACKGROUND

1.1 Introduction

Progress towards a sustainable energy economy requires not only the production of clean energy sources, but more sustainable means of organic waste disposal. Certain waste streams from food and agricultural processes, as well as municipal sludge contain substantial quantities of substrates which can be digested by anaerobic organisms into volatile fatty acids (VFAs). Microbial hydrogen production processes utilize the catalytic enzymes and light absorption processes found in certain microorganisms to generate hydrogen as a result of either water splitting from photophosphorylation or as a byproduct of nitrogen fixation[1].

Purple non-sulfur bacteria (PNSB) are able to utilize VFAs[2], sugars[3] and lignin monomers[4] as carbon sources, and use light energy to drive hydrogen production by the nitrogenase enzyme. In addition, because PNSB are able to absorb near-infrared (NIR) light, they can be preferentially stimulated in cocultures with other phototrophic bacteria which cannot utilize near-infrared light[5]. Although this process of photofermentation by PNSB is attractive due to the ability to utilize a wide range of substrates and capabilities of reaching high conversions of substrates to hydrogen, increasing the efficiency of converting light energy to hydrogen remains a challenge[1].

NIR LEDs are an attractive option for illumination as they can be selected to match the NIR absorption of PNSB. Additionally, LEDs are more power efficient than widely used broadband tungsten light sources[6]. Although some researchers previously found

improvements for targeting visible absorbance of PNSB around 590nm[7], works using NIR LEDs found different levels of improvements compared to broadband tungsten sources[6,8].

One potential method for increasing light utilization of photofermentation processes that has not been reported is to exploit the photonic properties of plasmonic nanoparticles. These nanoparticles, often made from noble metals like gold and silver, are characterized by the collective oscillations of free electrons at the metal surface at resonant frequencies[9]. Gold nanoparticles in particular have found wide use in biosensing, cellular imaging, cancer therapy, and solar-cell enhancements [10-13]. These localized plasmon oscillations enhance the electric near-field around the particle, and they strongly depend on the particle's material and the surrounding media.[14] Plasmonic nanoparticles also often exhibit absorption and scattering cross sections significantly greater than their cross-sectional areas. The combination of targeted illumination with scattering and near-field enhancement effects from plasmonic nanoparticles, see Figure 1.1, could serve to increase light utilization and improve hydrogen production in PNSB.

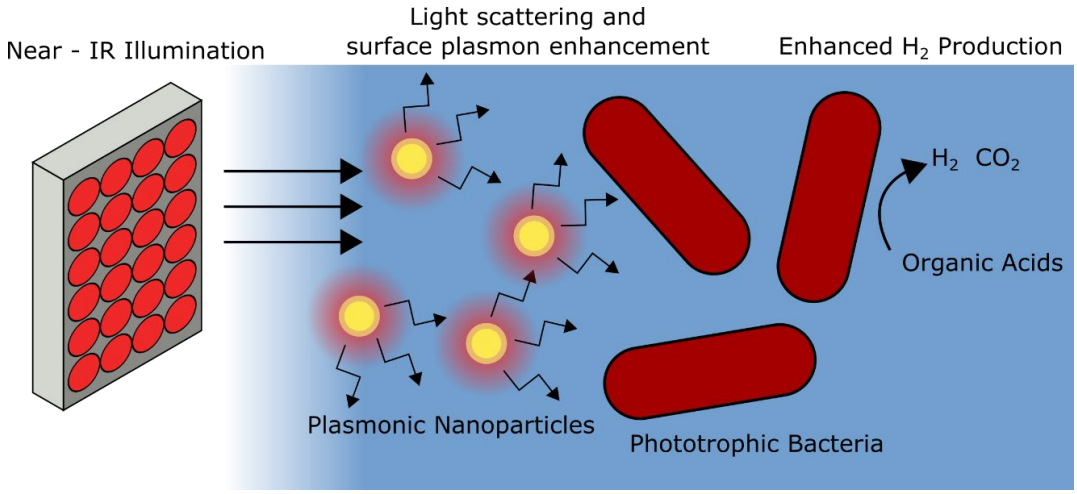

Figure 1.1 Combination of NIR light and plasmonic nanoparticles for hydrogen production form organic acids

1.2 Organisms for Hydrogen Production

PNSB are not the only organisms available for microbial hydrogen production; green algae, cyanobacteria, and certain dark fermentative bacteria such as members of the genus *Clostridium* are capable of substantial rates of hydrogen production[15]. All of these organisms are capable of enzymatic production of hydrogen from either hydrogenase or nitrogenase enzymes. Hydrogenase enzymes are widely spread across many microorganisms due to the critical need to control the proton motive force which can be used to drive important transmembrane proteins, including certain transport processes and the generation of ATP.[16]

Dark fermentative bacteria play an important role in microbial hydrogen processes. These organisms are capable of metabolizing a wide array of complex substrates and biomass, and the organic acids they produce from fermentation can be used to drive the

growth and hydrogen production in phototrophic organisms. These species produce hydrogen through the hydrogenase enzyme, and vary in their efficacy and whether or not they are reversible. Hydrogen production yields from dark fermentative are low, with the max around 33% of the expected H_2 production from glucose alone[17]. Nevertheless, these organisms could play an important role in waste stream processes.

Oxygenic phototrophic bacteria suitable for hydrogen production are primarily composed of two broad groups; cyanobacteria and green algae. Both groups have similar photocenters are capable of using water as an electron donor, generating oxygen in the process. Both of these groups are capable of hydrogen production from the hydrogenase enzyme, but only cyanobacteria also use the nitrogenase enzyme[18]. The metal cofactor of nitrogenase, usually iron or molybdenum, is oxidized and made inactive in aerobic environments[19]. Cyanobacteria deal with oxygen sensitive processes by forming heterocysts, specialized compartments to carry out anaerobic reactions. Under nitrogen starved conditions, transmembrane proteins selectively transport nitrogen across the gas impermeable membrane. Light conversion efficiencies form cyanobacterial heterocysts are typically lower than non-oxygenic phototrophic bacteria, less than 1% compared to ~1-10%, because the substrates used to drive energy production within the heterocyst must be supplied by nearby phototrophic cells.[17] Algae also face a limitation in hydrogen production due to oxygen production diminishing the activity of their reversible hydrogenase. Instead of spatially separating the processes like cyanobacteria, algae can be grown in a sulfur rich medium and transferred to a sulfur deficient medium for hydrogen production, since sulfur is needed to replenish damaged photocenters which oxidize water[20].

Purple non-sulfur bacteria are attractive organisms for microbiological hydrogen production because they can utilize unidirectional nitrogenase enzymes for hydrogen production like cyanobacteria, but they are not oxygenic. These organisms are capable of high substrate conversion to hydrogen (75%>) for suitable substrates.[1] Because light utilization is often seen as the primary challenge with PNSB, evaluating different lighting strategies should give valuable insight into how to improve the process.

1.3 Objectives

1. Describe modes of growth and the impact of illumination on purple non-sulfur (PNSB) growth and development.
2. Culture model PNSB *Rhodopseudomonas palustris* for use in hydrogen production from acetate and investigate strategies for developing photobioreactors
3. Compare use of targeted near-infrared illumination to widely used broadband illumination as a light source of hydrogen production by phototrophic PNSB using acetate as an organic substrate.
4. Investigate the effect of supplementing culture media for hydrogen production with optically resonant nanoparticles.

CHAPTER 2. BIOLOGICAL MECHANISMS OF PNSB AND GROWTH EXPERIMENTS

2.1 Introduction

The total process of photofermentation in PNSB passes through multiple critical steps to result in the production of H_2 from organic substrates. Light energy absorbed by the bacteria is harvested by light harvesting complexes and directed towards electron carrier reduction and generating proton motive force for ATP synthesis. These energetic molecules are used to drive nitrogenase activity in catalyzing the production of hydrogen under nitrogen limited conditions.[21] Meanwhile, CO2 produced from the degradation of VFA metabolites can also be fixed by the bacteria into biomass.[22] A better understanding of these processes helps to put photofermentation into perspective, and provides insight into proper culturing conditions. See Figure 2.1 for a scheme of important biopathways.

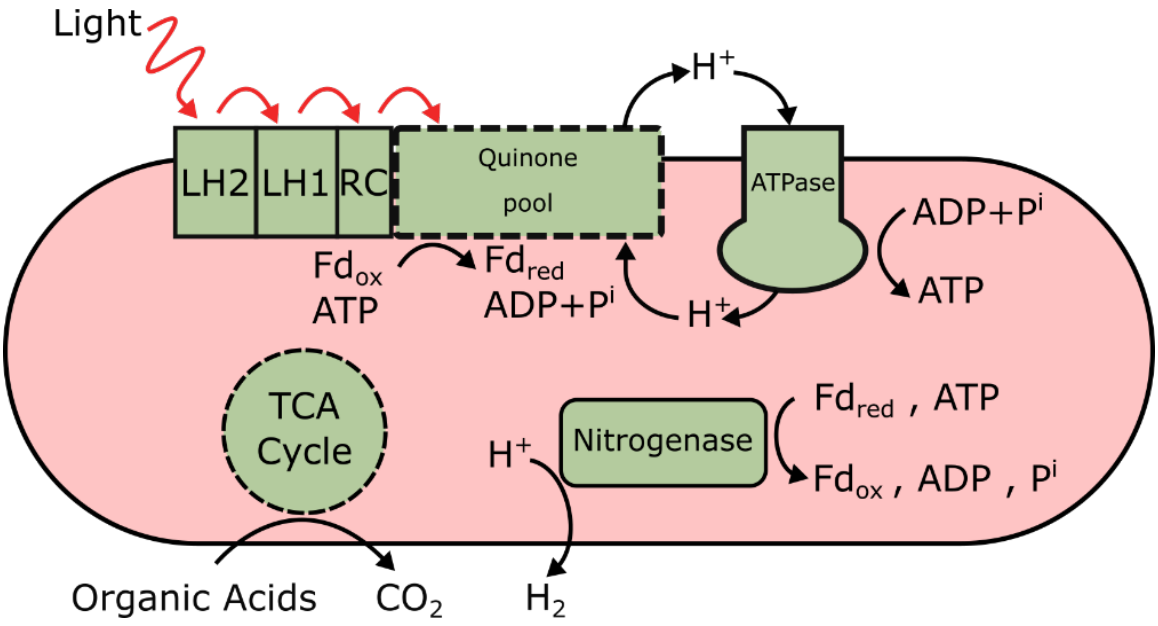

Figure 2.1: PNSB Biopaths for Photofermentation. LH2, LH1: light harvesting complex units. RC: reaction center. Fd_{ox}, Fd_{red}: ferredoxin electron carrier. P^i: inorganic phosphate. TCA: tricarboxylic acid cycle.

2.2 Light Harvesting Mechanisms

Light harvesting complexes located either on the bacteria membrane or on intracytoplasmic membranes, see Figure 2.1, are comprised of superstructures of pigments to absorb light energy and transfer it to a reaction center and subsequently into the electron transport chain. Each light harvesting complex has one transmembrane reaction center inside a primary ring of bacteriochlorophyll, the LH1 subunit. Satellite light harvesting subunits, LH2, surround LH1 and transfer energy through LH1 towards the reaction center.[23] In addition to near-IR absorbing bacteriochlorophyll, the light harvesting complexes also include carotenoids which serve both to harvest UV-visible light and protect the cell from the photoinhibitory effects of ultraviolet light.[24] Figure 2.2 Shows a schematic of the transfer from LH2 to LH1 and the reaction center RC.

Bacteriochlorophyll are typically labeled as B800 or B850 to signify the wavelength of maximum absorbance.

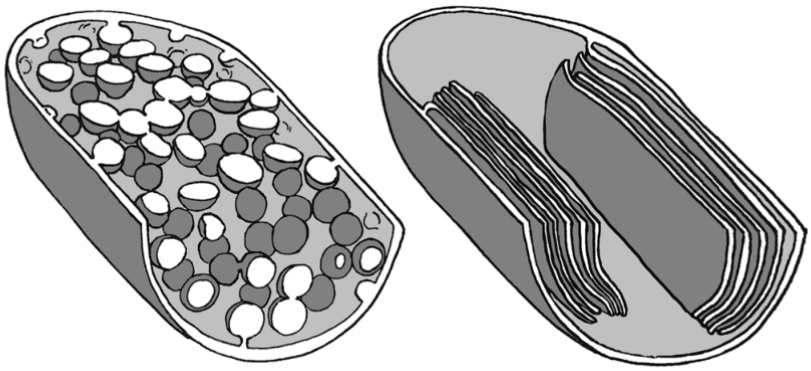

Figure 2.2: Intracytoplasmic Membranes (LaSarre 2018)[25] Left: Vesicular (*Rhodobacter sphaeroides*). Right: Lamellar (*Rhodopseudomonas palustris*) (*reprinted with permission from publisher*)

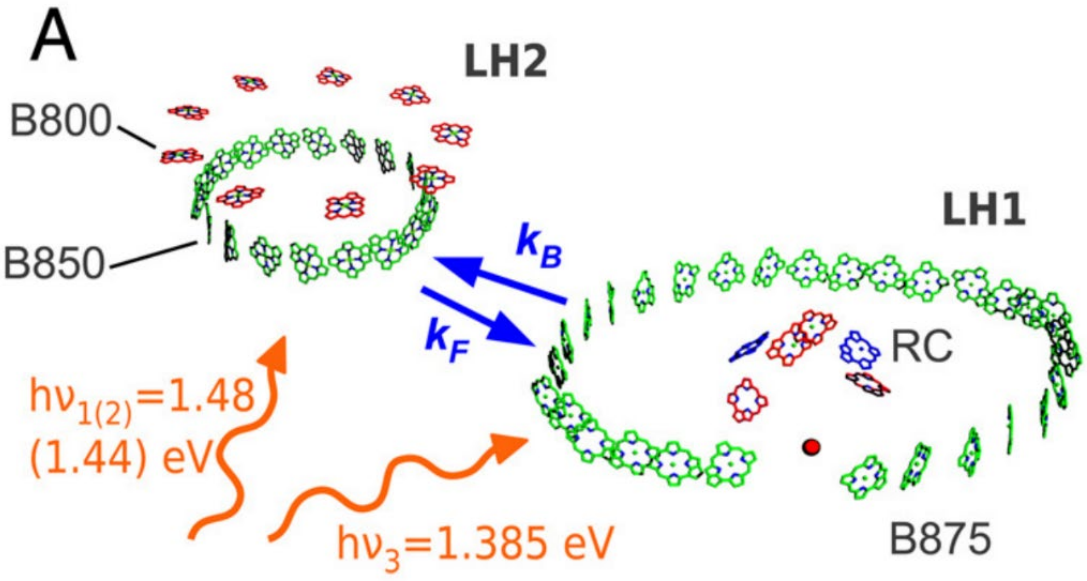

Figure 2.3: Light Transfer in a Light Harvesting Complex (Luer 2012)[23] (*reprinted with permission from publisher*)

Light harvesting complexes and the associated pigments do not grow constitutively in PNSB. Instead, only under illuminated, anaerobic conditions will bacteria develop characteristic red pigmentation associated with the development of light harvesting complexes. Additionally, energy absorbed from light spurs photoheterotrophic growth, which increases the growth rate compared to chemoheterotrophic growth in nutrient sparse medium.

To demonstrate these effects, 20 mL vials of minimal media, Defined Media 1 in Appendix 1, were inoculated with *R. palustris* and grown either under 2000 lux white LED or covered in aluminum foil and grown in the dark. Further, the growth curves were fit with a modified Gompertz model, shown in equation (5) below, to compare the effect of light intensity on cell growth.[26] The modified Gompertz model is a simple sigmoidal

growth model which has been expressed in terms of y, the cell density at time t (g/L); A, the maximum cell density (g/L); μ_m, the maximum growth rate (g/L/h); λ, the initial lag phase (h); and t, time (h). The data was fit using Matlab's fitnlm function, seen in Appendix 2.

$$y = A\exp\left(-\exp\left(\frac{\mu_m e}{A}(\lambda - t)\right) + 1\right) \qquad (5)$$

All model parameters, shown in Table 2.1, were significant with $p<0.05$. The increase in cell growth under illumination resulted in a 10x increase in the maximum growth rate and 6x increase in maximum cell density. Although the lag phase was shorter for cultures grown in the dark, this is likely due to noise at low cell density and the low maximum growth rate in dark cultures. Higher sampling rates in the initial growth period also made the noise at low cell densities have a larger impact on the model fit.

The final absorption spectrum shown in Figure 2.4b shows strong absorbance associated with bacteriochlorophyll at 590, 800, and 850-875nm. Carotenoid absorption is partially shown from 550-500nm, but not fully resolved. The dark spectrum, as expected, does not show any significant development of light harvesting complexes. An example picture of the final culture pigmentation is shown in Figure 2.5.

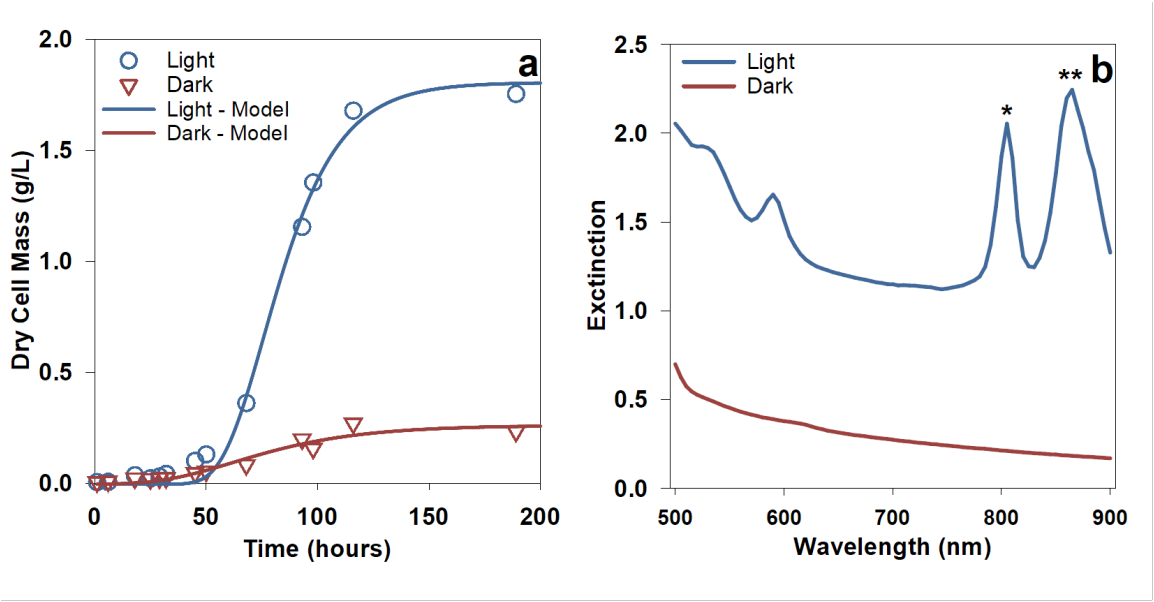

Figure 2.4: Cell growth and Spectra under Illuminated and Dark Conditionsa) Anaerobic growth of R. palustris in 20 mL minimal media at 30 °C using 70mM acetate as a carbon source and white LED (20 W/m2) for samples grown in light. Samples grown in dark covered in aluminum foil. Inset) Left to right: blank media, dark anaerobic growth, light anaerobic growth. b) Example extinction spectrum for R. palustris grown anaerobically under dark and light conditions after 90 hours. Bacteriochlorophyll (*) = B800 (**) = B850, B875

Table 2.1: Modified Gompertz Parameters y, the cell density at time t (g/L); A, the maximum cell density (g/L); μ_m, the maximum growth rate (g/L/h); λ, the initial lag phase (h); and t, time (h).

Mode	A (g/L)	μ_m (g/L/h)	λ (h)	adjR^2
Light	1.81	0.035	57.1	0.992
Dark	0.26	0.003	29.8	0.924

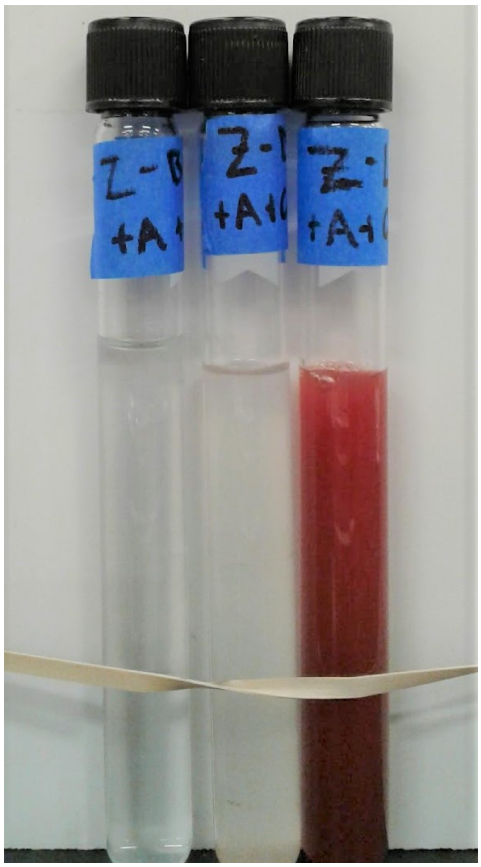

Figure 2.5: Culture Pigmentation Example

2.3 Nitrogen Fixation and Hydrogen Production

The production of hydrogen in PNSB is normally a side reaction of nitrogen fixation. Under nitrogen limited conditions, the nitrogenase enzyme reduces N_2 into NH_3 according to reaction (1). In the absence of N_2, nitrogenase acts only to produce H_2 reaction (2)[1]. This process is energy intensive and highly regulated; aerobic conditions or excess NH_3 result in downregulation of nitrogenase activity and reduced hydrogen production[19]. For this reason, PNSB grown for hydrogen production are often pregrown in a nitrogen rich medium for maximum growth rate, which can then be used as an

inoculant in nitrogen deficient medium to study hydrogen production.

$$N_2 + 8H^+ + 8e^- + 16\,ATP \rightarrow 2NH_3 + H_2 + 16ADP \quad (1)$$

$$8H^+ + 8e^- + 16ATP \rightarrow 4H_2 + 16ADP \quad (2)$$

2.4 CO2 Utilization

Photofermentation of organic acids produces both H_2 and CO_2 in varying amounts depending on the substrates used, shown in reaction (3) for acetate and reaction (4) for malate. Subsequent fixation of CO_2 by the Calvin cycle reduces the net rate of CO_2 production and results in biogas more concentrated in H_2 [2]. The Calvin cycle also serves as a competing process to hydrogen generation from nitrogenase activity, as both processes consume large amounts of reducing power within the cell. Mckinlay et al. compared TCA cycle and Calvin cycle fluxes in *R. palustris* mutants with and without nitrogenase activity and found that the Calvin cycle flux was significantly depressed when nitrogenase activity was high [22]. These electron sink processes have a secondary role in the metabolic activity of anaerobic phototrophs to help maintain redox homeostasis within the cell.

$$C_2H_4O_2 + 2H_2O \rightarrow 2CO_2 + 4H_2 \quad (3)$$

$$C_4H_6O_5 + 3H_2O \rightarrow 4CO_2 + 6H_2 \quad (4)$$

In addition to the Calvin cycle, CO_2 production from PNSB is suppressed during growth using certain VFA substrates, notably acetate, because the TCA cycle shifts towards the glyoxylate shunt. This process results in reduced CO2 and NADH output, but enables the organism to assimilate short chain organic acids into biomass. The glyoxylate shunt is also preferred during growing stages of the culture, and nongrowing cultures have been shown to have higher TCA cycle fluxes. Sustained hydrogen production from non-growing cultures has been suggested to be due to excess reducing power generated from the shift towards TCA cycle in non-growing cultures[21].

To test the extent of CO_2 production we compared H_2 and CO_2 production using malate as a carbon source, seen in Figure 2.4. The final cumulative ratio of H_2:CO_2 was indeed lower than expected, with experimental results showing a ratio of 36:1 compared to the expected yield of 3:2, see reaction (4). As the CO_2 production remains low throughout the culture growth phase, it is likely that CO_2 production is repressed both by the predominance of the glyoxylate cycle over the TCA cycle, and some degree of subsequent fixation of CO_2 from the Calvin cycle. Likewise, many researchers have reported low CO_2 concentrations in biogas from PNSB hydrogen production from VFAs, with Turon et al. claiming the evolved gas was 97-99% H_2 [8].

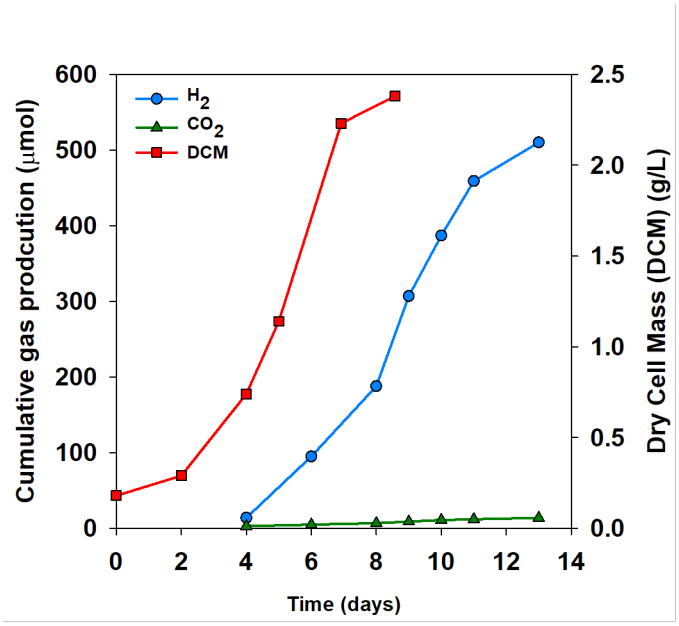

Figure 2.6: H_2 and CO_2 Profile Using Malate as a Carbon Source.300mL cultures of *R. Palustris* grown anaerobically at 22 °C using 850nm LED array illumination adjusted to 82-91 W/m2. 70mM malate was used as a carbon source. For each measurement the headspace was flushed with N_2.

2.5 Conclusions

Understanding the metabolic processes driving PNSB is a critical first step to improving the process, and gives some insight into standard practices for culturing PNSB. Because light harvesting complexes necessary for hydrogen production only develop under sufficient illumination, cultures are typically pregrown under light before inoculation of cultures for experiments. This ensures that experimental cultures have already adapted to develop light harvesting complexes, and controls for the time it would otherwise take for cells to adapt to illuminated conditions. The utilization of CO_2 by the bacteria is also an exciting result of metabolic activity that serves to enrich the produced biogas from photofermentation.

CHAPTER 3. CULTURING PURPLE NON-SULFUR BACTERIA

3.1 Introduction

Hydrogen production from purple non-sulfur bacteria requires appropriate culturing media and reactor setup to establish a suitable anaerobic environment. Additionally, comparing the effects of different light sources on photofermentation from PNSB requires accurate quantification of culture densities, hydrogen concentrations, and light intensities. This chapter covers microbiological and analytical techniques used in this work as well as considering potential improvements for photobioreactors for future work.

3.2 Media Selection

R. Palustris (CGA 009) cultures were grown using various media types at the outset of the project to select growth conditions for further experiments. Complex media types suggested by ATCC [27] provide a rich media for pregrowth of bacterial cultures, but preclude certainty in the molecular source of carbon and nitrogen due to the use of yeast extract or soy broth. Defined media types are used either to control the specific nutrients used by microbes or as a means of limiting contamination. Further for metabolically versatile organisms like *R. Palustris* the media content determines not only the efficacy of growth, but whether or not the organism grows in a phototrophic / chemotrophic or heterotrophic / autotrophic domain. Complex media types with excess fixed nitrogen in particular are useful for pregrowth of bacterial cultures, but this fixed nitrogen content results in downregulation of nitrogenase activity required for hydrogen production.

Growth from various media types, see recipes in Appendix 1, is shown in Figure 3.1 for cultures illuminated with white LED, and in Figure 3.2 for cultures grown in the

dark. Complex media types 1 and 2 resulted in the shortest lag phase, which was expected for rich complex cultures. Complex type 3 showed little growth, likely due to a low concentration (0.2 g/L) of yeast extract. Both defined media types showed increased lag phase, but Defined 1, which was chosen for hydrogen production experiments, resulted in a higher cell density. Notably only complex media types 1 and 2 showed significant growth without illumination, indicating that these media types were able to sustain chemotrophic growth.

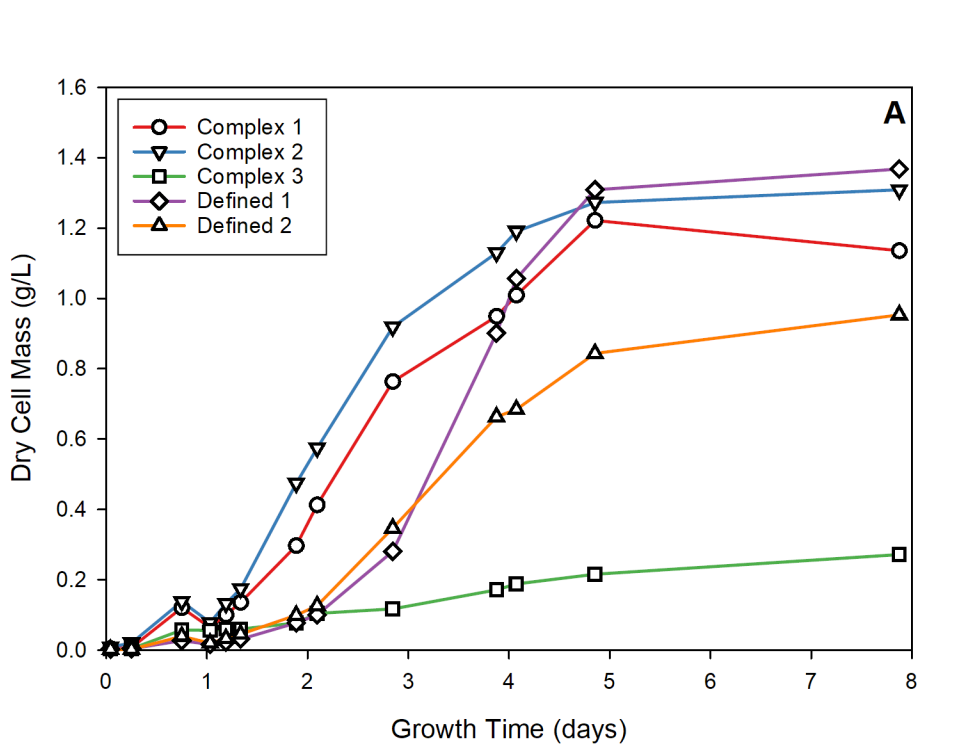

Figure 3.1: Growth in Various Media - Light. 20mL culture vials of *R. palustris* in various media, illuminated with 2000 lx white LED. For recipes see Appendix 1.

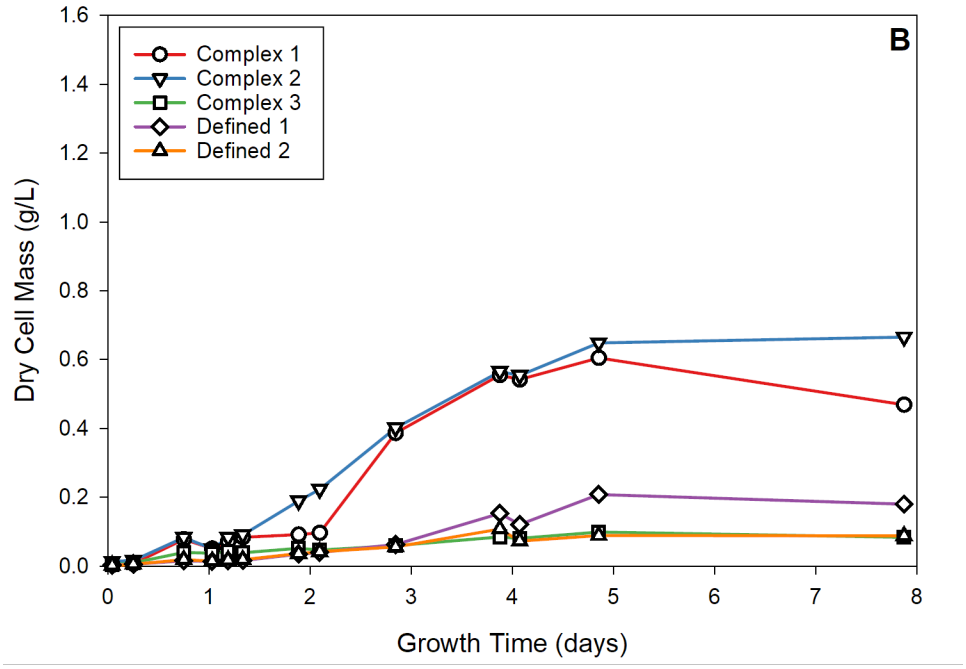

Figure 3.2: Growth in Various Media – Dark. 20mL culture vials of *R. palustris* in various media, illuminated with 2000 lx white LED. For recipes see Appendix 1.

3.3 Culture Preservation

Bacteria are able to adapt to different environments, incorporate plasmids into their genetic code, and accumulate mutations of many generations. In order to ensure adequate replicability of experiments using microbiological organisms it is important to preserve cultures for future use. A flowchart of efforts taken to maintain culture purity for experiments is shown in Figure 3.3.

Rhodopseudomonas palustris CGA 009 was obtained from ATCC in a freeze dried powder form. The resuspended culture was then used to inoculate petri dishes of tryptic soy agar using a streaking technique to isolate single cultures. Isolated bacterial cultures from these plates are assumed to be the exact strain sent by ATCC, which are then used to inoculate and grow liquid cultures. From here, liquid cultures could either be

used to inoculate other agar plates to save for future experiments or used to make freezer stocks for long term storage. Freezer stocks were made by adding glycerol up to a final concentration of 20% glycerol. This freezer stock can be separated into small freezer tubes and stored in a -20 °C freezer and used to inoculate cultures for future experiments.

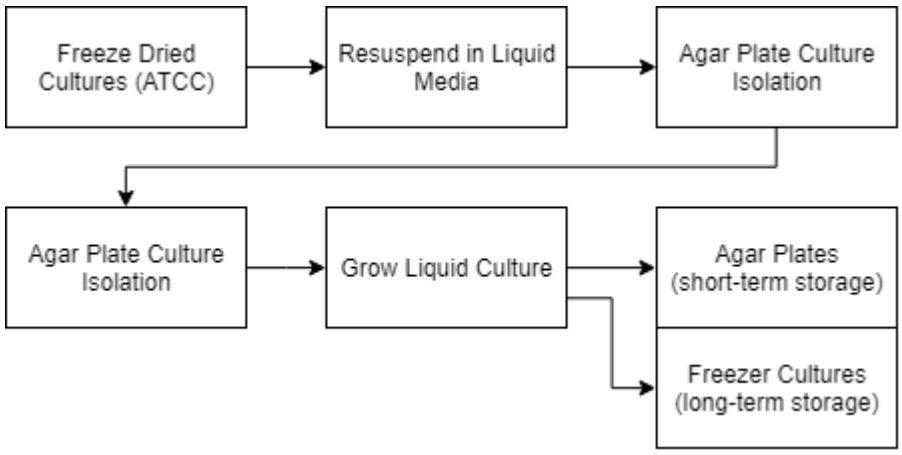

Figure 3.3: Culture Preservation Flowchart

3.4 Analytical Methods

3.4.1 H_2 and CO_2 Analysis

Hydrogen gas produced in photofermentation experiments was quantified by using a GC (Agilent 6890N) with a Carboxen-1004 micropacked column (0.75 mm × 2 m) equipped with TCD detector. The column temperature was hold at 50 °C for 1 min, then raised to 150 °C at 10 °C /min and kept for 5 min. Nitrogen was used as the carrier gas at 1.8 ml/min. The injector and the detector temperatures were set at 100 °C and 150 °C, respectively. The retention times for hydrogen gas was 1.3 min. A calibration curve was obtained for hydrogen gas in the linear range of 100-1000 ppm, shown in Figure 3.4.

Helium is often used as a carrier gas for detection of light hydrocarbons and other gasses using a thermal conductivity detector, but the best sensitivity is obtained when the carrier gas and analyte have very different thermal conductivities. Helium and hydrogen both have high thermal conductivities, so nitrogen was used as a carrier gas. For the analysis of CO_2, the same method was used and a two-point calibration between 200 and 400 ppm was used for analysis.

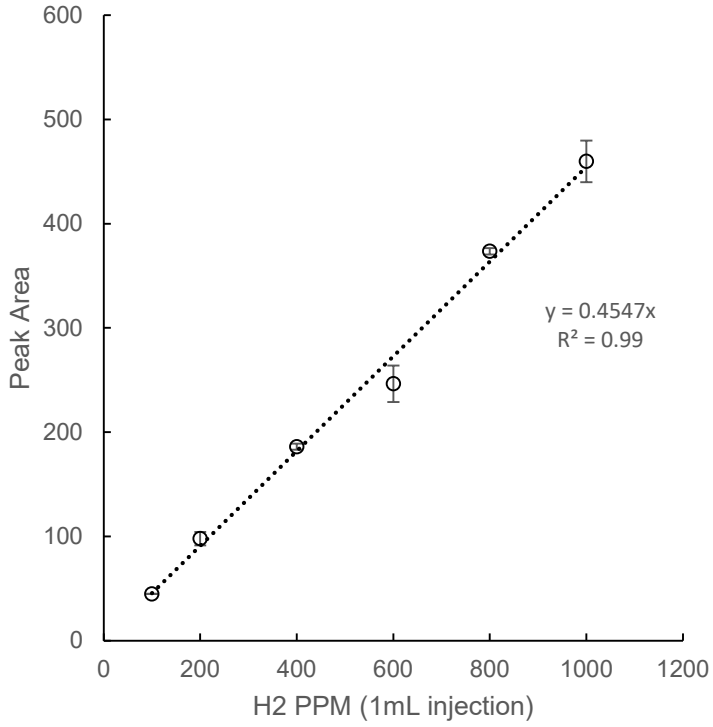

Figure 3.4: Hydrogen Thermal Conductivity Calibration Curve

3.4.2 Cell Density Measurement

Cell density measurements are typically reported as dry cell mass (DCM g/L). Because the drying and weighing of bacterial cultures is laborious, it's common to make a calibration curve with optical absorbance at a selected wavelength to quantify cell

density. In this case we used the absorbance at 660nm (optical density 660nm or OD660nm) because it represented a flat region of the spectrum that would not be conflated with bacteriochlorophyll absorbance. A dense culture of *R. palustris* was serially diluted, and the optical density measured using a BioTek microplate reader (Synergy H1 Hybrid reader). Simultaneously, multiple aliquots of the dense culture in pre-weighed glass vials were gently dried in a vacuum oven at 80 °C until there was no mass change. The resulting calibration curve is shown below in Figure 3.5. The optical density is presented as the optical density minus that of the medium alone so that the calibration curve can be used for different media types.

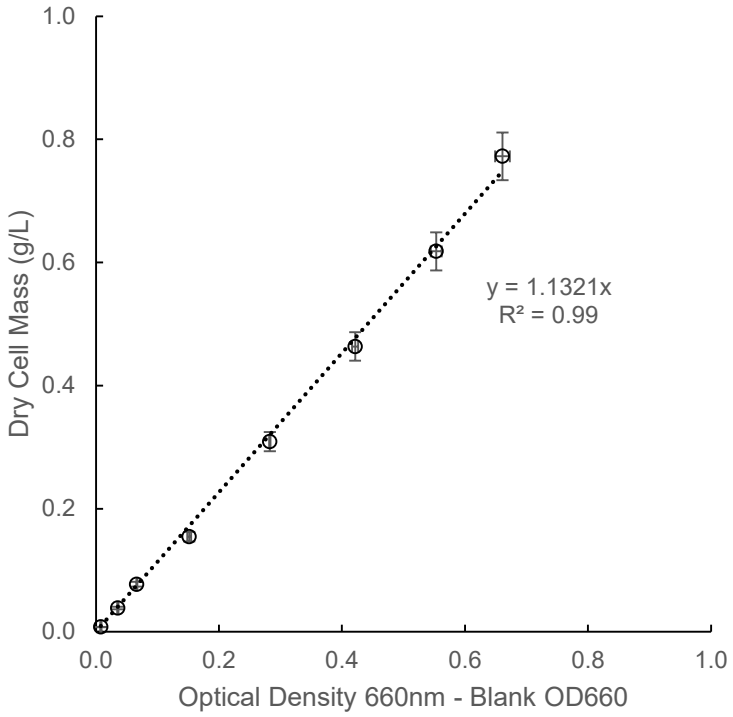

Figure 3.5: Cell Density Calibration Curve

3.4.3 Light Measurement

The spectrum of both light sources (broad wavelength EVA 64623 bulb OSRAM HLX 100w single ended tungsten – halogen bulb and NIR-LED source, CM-Vision CM-IR110 LED array) was measured with an Ocean Optics HR4000CG-UV-NIR spectrophotometer, shown in Figure 3.6. Note that the NIR source overlaps with the bacteriochlorophyll absorption maxima shown in Figure 2.4. The broadband tungsten light source has little UV content, but the results of this graph may underrepresent the infrared content, as the spectrophotometer was not calibrated for long wavelength sources. Regardless this broadband source has high intensity visible light content, and overlaps with the absorption of R. palustris at 590nm as well as the carotenoid absorption, but is not concentrated on bacteriochlorophyll like the NIR source.

The light power was measured using light power meter (LabMax-TOP, Coherent Inc.). For vial experiments the light intensity was measured at the bottom face of each illuminated vial. ??? shows the result of intensity measurements from the light same light sources in ??? after the intensity of both lights was adjusted to 140 W/m^2. Although the central tendency of both light intensities is close to 130, the broadband tungsten source has significantly higher variance in intensity due to the geometry of a single light illuminating a flat surface area. On the other hand, the NIR-LED array had a surface area close to the surface area illuminated, so the intensity was more tightly controlled.

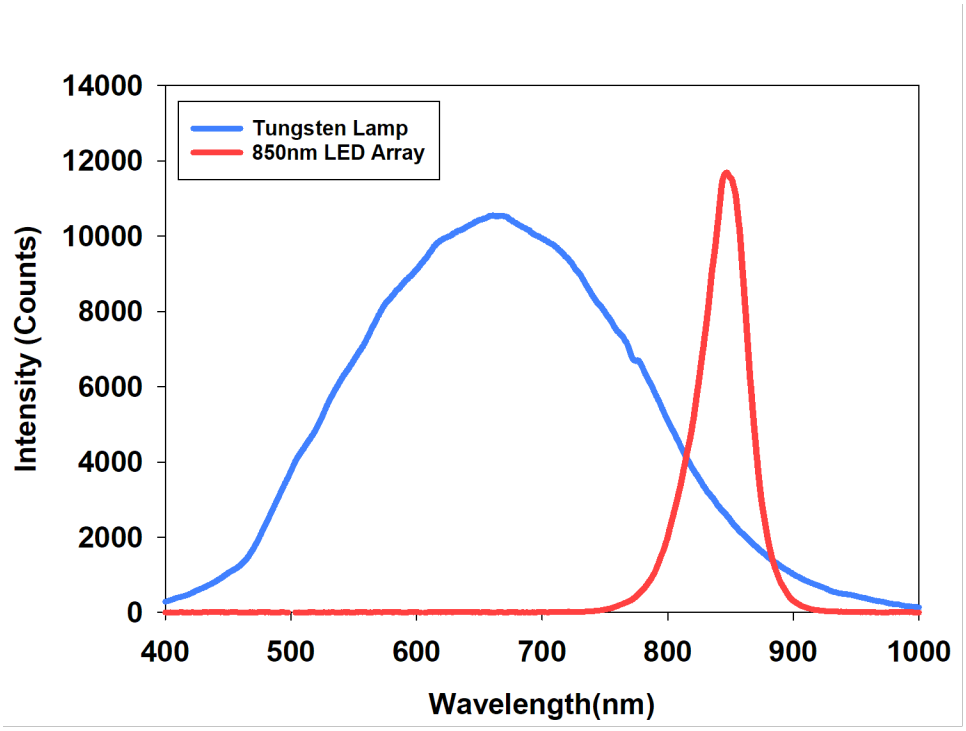

Figure 3.6: Spectra of Broadband tungsten and NIR-LED Array

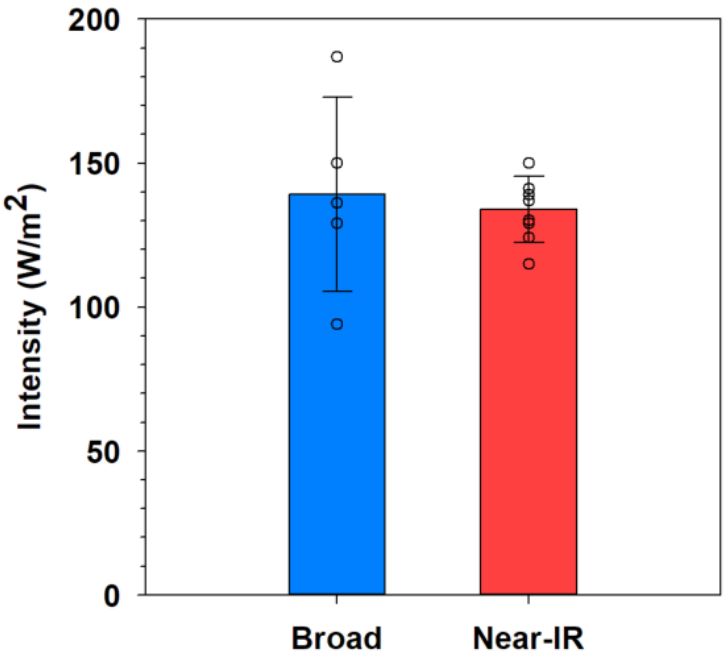

Figure 3.7: Intensity Variance of Broadband Tungsten Lamp and NIR-LED Array

3.5 Lab Scale Photobioreactor Selection

Hydrogen production experiments using photobioreactors can be set up in a few different ways to collect and analyze biogas. Each reactor must be able to establish an anaerobic environment for hydrogen production, and allow sufficient illumination to grow the bacteria. This section lists some pros and cons of different gas collection methods. The 3 different types of collection systems are shown in Figure 3.8.

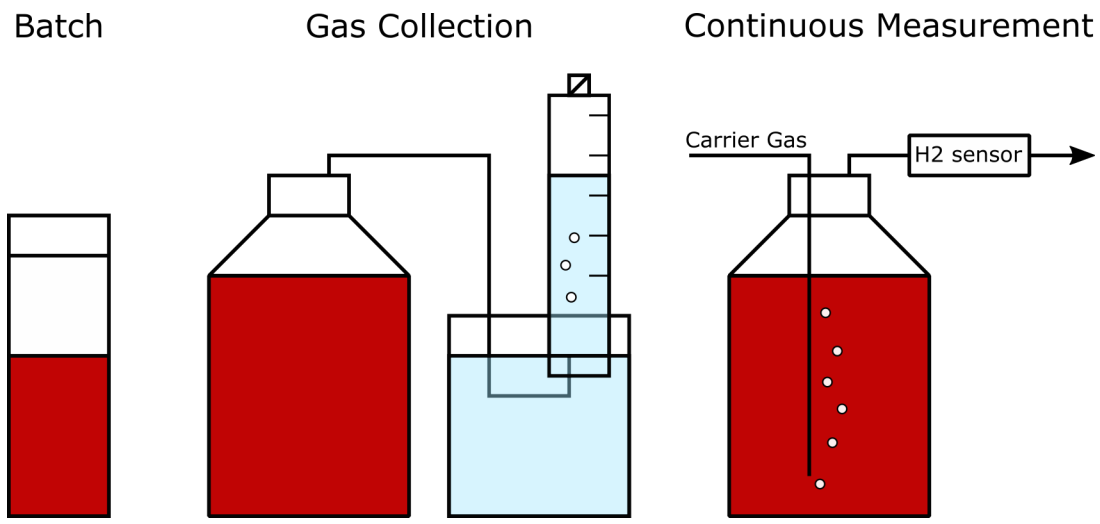

Figure 3.8: Different Types of Gas Measurement from Photobioreactors

3.5.1 Batch Vials

Batch cultures of purple-nonsulfur bacteria are perhaps the most ubiquitous gas collection method in literature. We chose to use batch cultures as a primary method for light comparisons because of the ease of replication. These culture vessels may be glass vials or flasks, and are usually plugged with a septum. To quickly establish an anaerobic environment, it is best to either sparge the culture media or flush out the headspace with nitrogen or argon before growing the bacteria.

The primary concern with this method is that hydrogen may escape through the septa during the course of the experiment, especially if pressure builds up in the vessel. Thicker butyl rubber septa are often used in literature as one way to diminish this risk. The septa may be damaged if punctured multiple times during an experiment to acquire gas generation profiles. Additionally, all purple non-sulfur bacteria are capable of

utilizing hydrogen as an electron donor, so the hydrogen may be consumed at high concentrations.

3.5.2 Biogas Collection Reactors

Gas collection columns coupled to a photobioreactor can be used to collect hydrogen outside of the photobioreactor. Because hydrogen has a low solubility in water, the biogas generated can be bubbled into a water displacement column, and the volume of gas produced can be measured over time. The setup in Figure 3.9 shows the basic setup, although this particular setup was not sufficiently hydrogen impermeable to use for light comparison experiments. Future efforts could use inverted stoppered graduated cylinders to capture biogas, and more hydrogen impermeable Viton tubing to connect to the reactor[28].

One concern of this method is the quantification of other components of the biogas. CO_2 can dissolve in water and build up carbonic acid, which may artificially increase the H_2 content of the biogas. This can be addressed by either collecting over an acidic medium to retain CO_2 or by passing the biogas through a strong basic solution to absorb CO_2 before retaining the biogas.

An example run of the gas collection setup can be seen in Figure 3.10, which was able to resolve a sharp increase in biogas production during the growth phase and decreased production as the media substrate was consumed.

Figure 3.9: Photobioreactor with Gas Collection Column

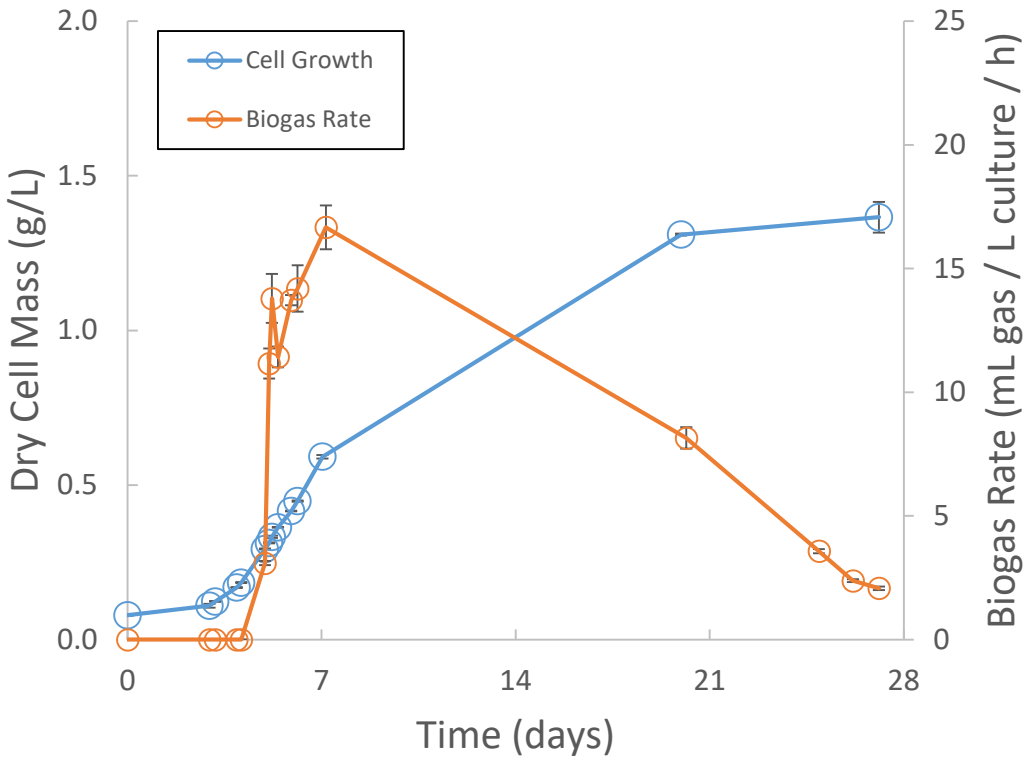

Figure 3.10: Biogas Collection Reactor Trial

3.5.3 Continuous Gas Measurement Reactors

Continuous measurement reactors use a carrier gas to push evolved hydrogen and CO_2 towards a measurement device. The measurement source can either be a dedicated detector, such as an electrochemical sensor, or an auto-sampler to a GC. Continuous measurement of the gas stream from a bioreactor can potentially provide a great deal of information, but requires a more sophisticated reactor setup and is rarely used in literature.

Electrochemical sensors can provide rapid hydrogen analysis within certain limitations. A typical scheme for an amperometric electrochemical sensor is shown in Figure 3.11. Hydrogen in a carrier stream diffuses across a membrane, and into an electrolyte. The sensing electrode is held at a constant voltage, and changes in current due to hydrogen oxidation are used to determine hydrogen concentration in the carrier stream. This offers fairly rapid analysis, but is sensitive to changes in the carrier gas temperature, pressure, and humidity. Additionally, cross sensitivity with other hydrocarbons can lead to varying results if the gas composition changes.[29,30]

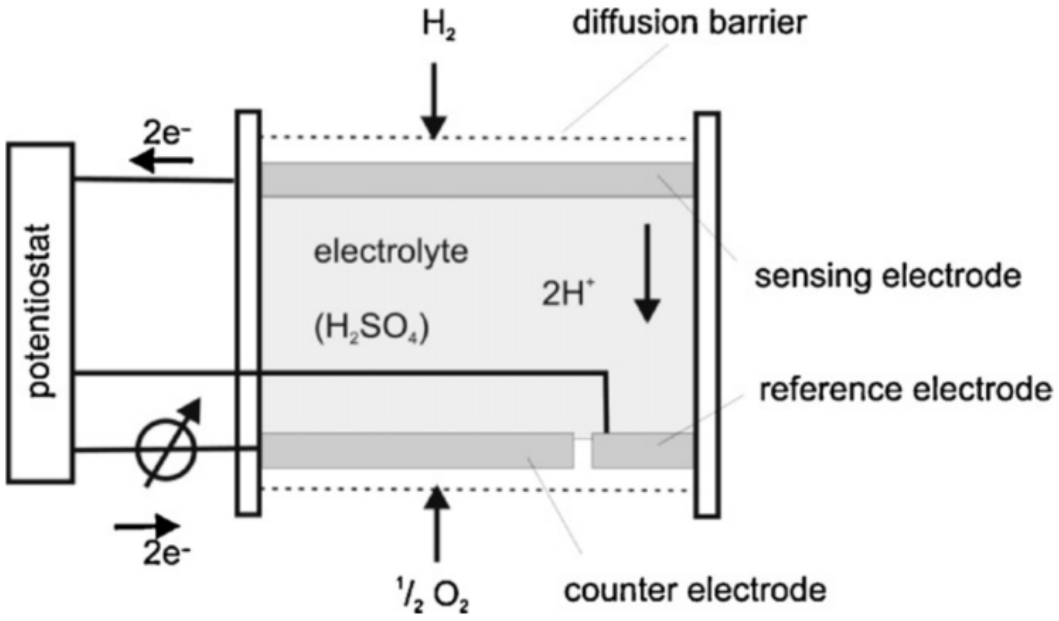

Figure 3.11: Amperometric H_2 sensor (Hubert 2011). *(reprinted with permission of the publisher)*

CHAPTER 4. ENHANCEMENT OF HYDROGEN PRODUCTION FROM NEAR-INFRARED ILLUMINATION

4.1 NIR enhancement of Hydrogen Production

We were interested in determining if the illumination of a NIR source alone results in increased hydrogen production for *R. palustris*. Shifting illumination into more preferentially absorbed portions of the spectrum should increase the amount of energy available to the bacteria. To determine the effect of shifting the wavelength of illumination, parallel batch cultures of 35mL in 40mL septa vials were grown using two different light sources; a broad tungsten source and a NIR LED array centered around 850 nm, seen in Figure 4.1. The spectra and variance of intensity of these light sources can be found in Figure 3.6 and Figure 3.7. Culture media used for these experiments can be found under Defined Media 1 in Appendix 1, using 70mM acetate as a carbon source and 7mM glutamate as a nitrogen source.

Cultures illuminated with NIR LEDs produced almost 3 times more hydrogen than those illuminated with a broad light source. This is expected at light intensities below a saturation limit; shifting illumination into preferentially absorbed regions of the electromagnetic spectrum should increase available energy and reductive potential within the bacteria and increase metabolic activity. Increased metabolic activity also resulted in an increase in cell density, with cultures illuminated with NIR LEDs reaching a final cell concentration 1.5 times higher than those illuminated with a broadband light source.

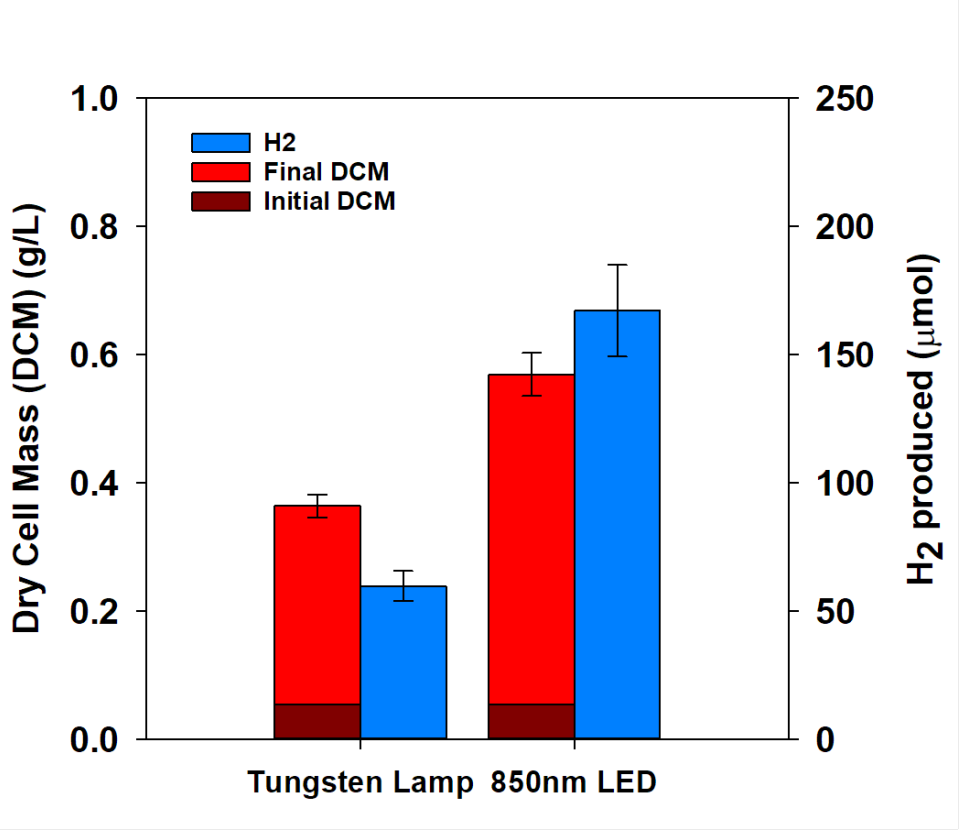

Figure 4.1: Enhancement of Hydrogen Production from NIR Illumination in Batch Vials Batch growth, 40mL PTFE/silicone septa vials illuminated with NIR LED array (850 nm) or a Tungsten Lamp (peak 660 nm, broad) for 90 hours at an intensity of 130 W/m2. n = 4 vials per illumination source. All vials incubated at 30° C and shaken at 100 RPM in an orbital shaker.

To further describe the efficacy of targeted illumination for increasing hydrogen production in PNSB we compared the effect of switching light sources on a single pregrown culture. Figure 4.2 shows the results of pregrowing a 300mL culture of *R. palustris* in a cylindrical membrane reactor under broad illumination, switching to NIR LEDs of matched intensity, and switching back to broad illumination. Each measurement of hydrogen represents 3 samples from the headspace of one reactor after gas collection for 24 hours. The culture density increased 40% over the entire measurement period, but

hydrogen production was around 3.5-5x higher under NIR LED illumination. Increases are comparable to those in Figure 3a despite the increased culture size. This shows that the increases in hydrogen production efficiency under NIR LEDs was not solely due to an increase in culture density.

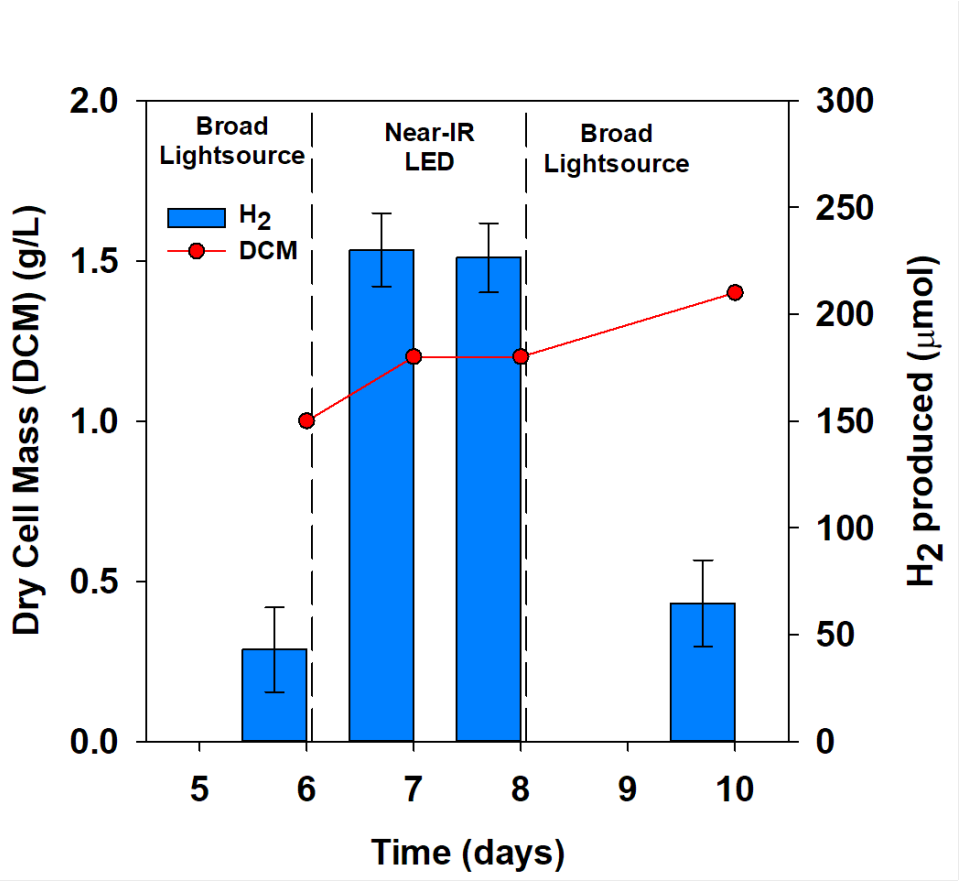

Figure 4.2: Enhancement of Hydrogen by Switching Light Source of 300mL Culture. *R. palustris* cultured in a 300 mL reactor using 70mM acetate as a carbon source under a broadband tungsten light source and then switched to illumination using an 850 nm LED array for 2 days and switched back to the broad light source. Illumination intensity for both sources was adjusted to the range of 82-91 W/m2, cultured at 22 °C. Hydrogen production accounts for headspace collection over 24h. n = 3 headspace measurements

Similar comparisons of using NIR illumination had varying results. Kawagoshi et al., using a 200 mL culture of *Rhodobacter sphaeroides*, found that illumination with a 2000 lux NIR LED resulted in a higher initial growth rate and hydrogen production rate compared to a 8000 lux tungsten bulb (about 2x more hydrogen production from NIR LED after the first 100 hours).[6] This resulted in about 2x more hydrogen production for the NIR illuminated culture after the first 100 hour, but only 1.3x increase in cumulative hydrogen production over the entire course of the experiment.

Our results are in contrast to those presented by Turon et al., who found that NIR illumination only resulted for around half of the total hydrogen production of a 1L culture of *Rhodobacter capsulatus* compared to incandescent (300-1100nm) illumination. They attributed the drop in performance to self-shading effects; the NIR light was preferentially absorbed at the illuminated surface of the container, leaving deeper parts the culture under-illuminated and decreasing the total hydrogen production.[8] In contrast, our experiments used a smaller culture size, 30 mL compared to 1 L, and lower intensity illumination, 130 W/m^2 compared to 1150 W/m^2. A smaller culture size could diminish the effects of self-shading, and lead to the reversal in efficacy of NIR illumination shown in These results underscore that effective light distribution within the culture is critical for maintaining hydrogen production, particularly in dense cultures.

CHAPTER 5. ENHANCEMENT OF HYDROGEN PRODUCTION FROM PLASMONIC NANOPARTICLES

5.1 Localized Surface Plasmon Resonance

Localized surface plasmons are collective oscillations of free electrons that lead to charge oscillations on the surface of nanostructures. These oscillations can be driven by optical photons, particularly those with wavelengths near the localized surface plasmon resonance (LSPR). The resonance wavelength can be tuned by changing the geometry and optical properties of the nanoparticle as well as the properties of the surrounding media.[14] On resonance, localized surface plasmon oscillations enhance the electromagnetic near-field around the particle and increase both absorption and scattering cross-sections. In many cases, the absorption and scattering efficiencies, the ratio of optical to physical cross section, can exceed one. Nanoparticles exhibiting LSPR have widely been studied for applications including solar cells, drug delivery, pollutant degradation, and affinity sensing.[10,31-40] Both near-field enhancement and light trapping through efficient scattering from these nanoparticles can improve the efficiency of light harvesting systems.

Our innovative approach utilizes nanoparticles with localized surface-plasmon resonance wavelengths around the NIR absorption maxima of bacteriochlorophylls. Specifically, we use nanoparticles with a silica core and a gold shell, an example of which is shown in cross section in Figure 5.1.[41,42] These core-shell particles enhance the optical near-field potentially leading to more efficient coupling to light-harvesting complexes in the bacteriochlorophylls. In addition, they offer relatively high scattering cross-sections with relatively low absorption cross-sections as discussed in the

supplementary information. This property enhances light trapping in the reactor due to efficient scattering while reducing light lost to particle absorption.

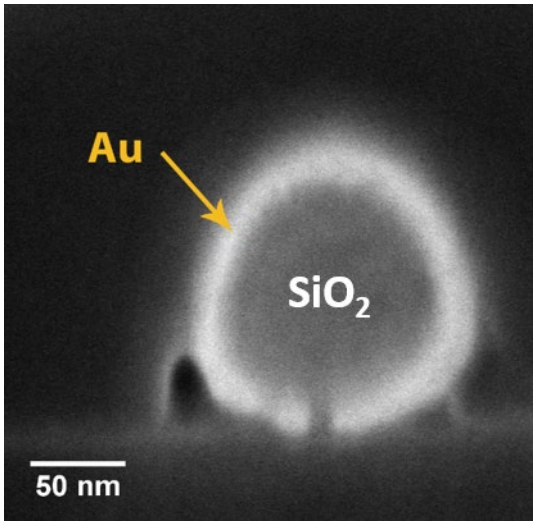

Figure 5.1: Gold-Silica Core-Shell Nanoparticle Cross Section.Shell thickness ~18nm.

5.2 Nanoparticle Selection and Characterization

Preliminary particle selection was based on Mie theory calculations of optimum extinction cross section area at the NIR region.[43] The optimum particles were silica-gold core-shell structures (~160 nm silica core, ~18 nm gold shell). These particles have broad extinction peak around 850 nm that is primarily due to scattering, see Figure 5.2. Other shapes of particles will also serve the purpose such as nano-rods[44], rings[45], and cages [46],or various passivated copper structures.[47] The experiments conducted here used particles with a nominal silica core diameter of $120\ \text{nm} \pm 9\ \text{nm}$, a gold shell diameter of 16 nm, a 5kDa mPEG coating, and a total diameter of $151\ \text{nm} \pm 8\ \text{nm}$ (NanoXact from nanoComposix Inc.) The cross-sectional electron micrograph in Figure 5.1 reveals the core-shell structure.

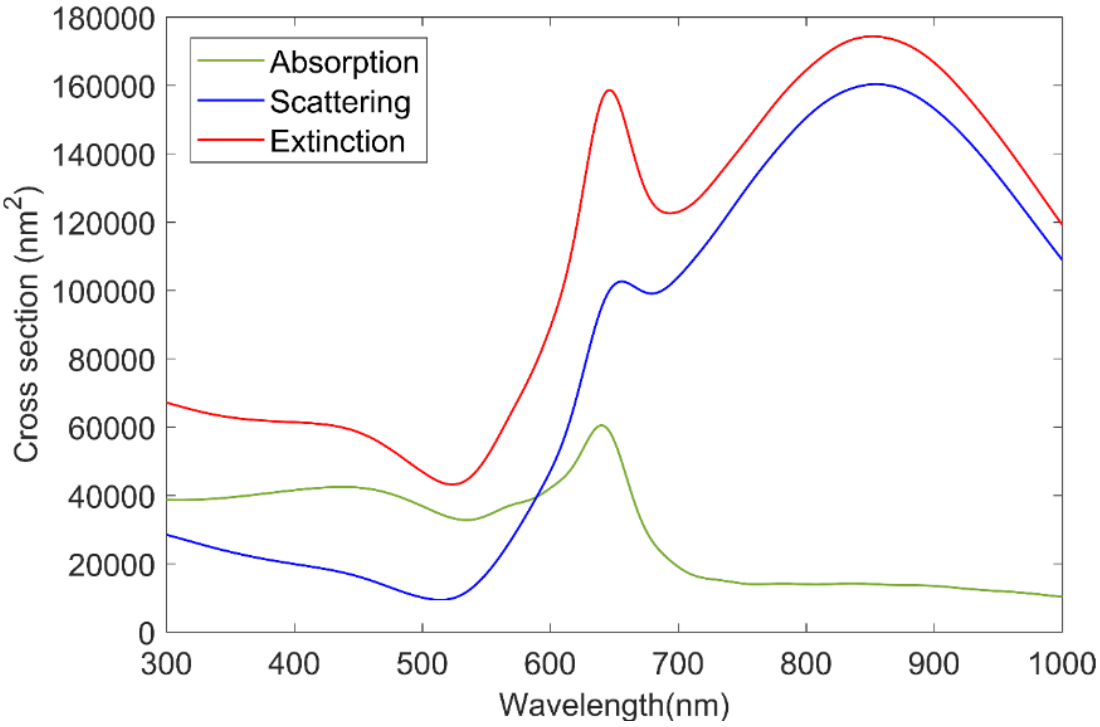

Figure 5.2: Simulation of Absorption, Scattering, and Extinction Cross Section of Gold-Shell Nanoparticles. FDTD simulation results for optimum silica-gold core-shell particles with resonance wavelength at 850 nm. The extinction cross section represents the sum of absorption and scattering. The diameter of the core is 120 nm and thickness of shell is 18nm.

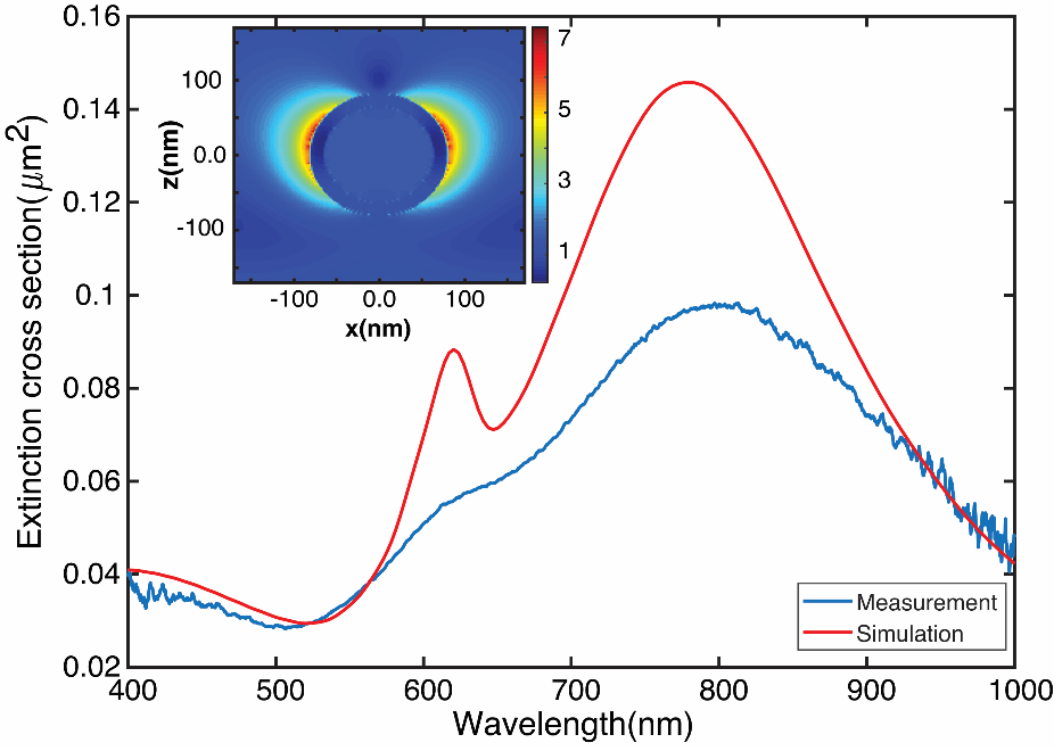

Figure 5.3: Simulated and Measured Extinction of Gold-Shell Nanoparticles. Inset shows simulated near-field electric enhancement around the nanoparticle

Figure 5.3 shows the calculated and measured extinction cross section of these particles which is dominated by scattering as noted above. Calculations were conducted using the finite difference time domain method and are detailed in the supplementary information. As expected, the broad extinction maximum associated with the LSPR is centered at 800nm and spans both of the NIR bacteriochlorophyll absorption maxima. The measured and calculated spectral shapes are similar and both the antisymmetric (~600 nm) and symmetric (~800 nm) resonances are apparent. The experimentally measured resonances are broadened and damped compared to the calculated resonances likely because of geometric heterogeneity and aggregation of some particles in solution. The calculated field enhancement around the particle is shown inset in **Figure 5b**. The

maximum field enhancement is 7× and the near-field decays over a distance of approximately 30 nm from the particle's surface.

These particles exhibit the desired near-field enhancement and efficient scattering near the bacteriochlorophyll extinction maxima. Thus, an experiments was conducted to quantify the enhancement of hydrogen production by R. palustris in the presence of gold nanoparticles. In this experiment, nanoparticles were dosed into samples at a concentration of 4.6 μg/mL (equivalent to 2.6×10^8 particles/mL).

5.3 Enhancement of Hydrogen using Gold-shell Nanoparticles

Improvements to light utilization in prototrophic bacteria have in the past included efforts to augment the production of certain pigments or adding synthetic light harvesting complexes[48]. Plasmonic materials have been shown to be able to couple to extracted light harvesting complexes from plants and bacteria as well, usually using extended gold arrays [49-51]. The results of Tsargorodska et al. are particularly interesting as they demonstrated strong coupling between extracted wild type light harvesting complexes of *R. sphaeroides,* another PNSB, and plasmonic gold nanostructure arrays.[51] This does not usually include live bacteria, however, and plasmonic nanoparticles have not in the past been shown to increase light utilization in phototrophic bacteria.

To test the efficacy of these nanoparticles for enhancing light absorption of *R. palustris*, cultures were gown under NIR LEDs with gold nanoparticles in solution, shown in Figure 5.4. The addition of nanoparticles resulted in similar cell growth, but more than 2× increase in hydrogen production over 90 hours. This is in addition to enhancements

from illumination with NIR LEDs. Although gold nanoparticles have been studied as a means to kill cancer cells through photothermal conversion[52,53], cell growth was not impeded here from the addition of nanoparticles because the intensity of light used is small compared to light intensity typically used for cancer treatment. Additionally, the 5kDa mPEG coating serves as a barrier between the nanoparticles and bacteria.

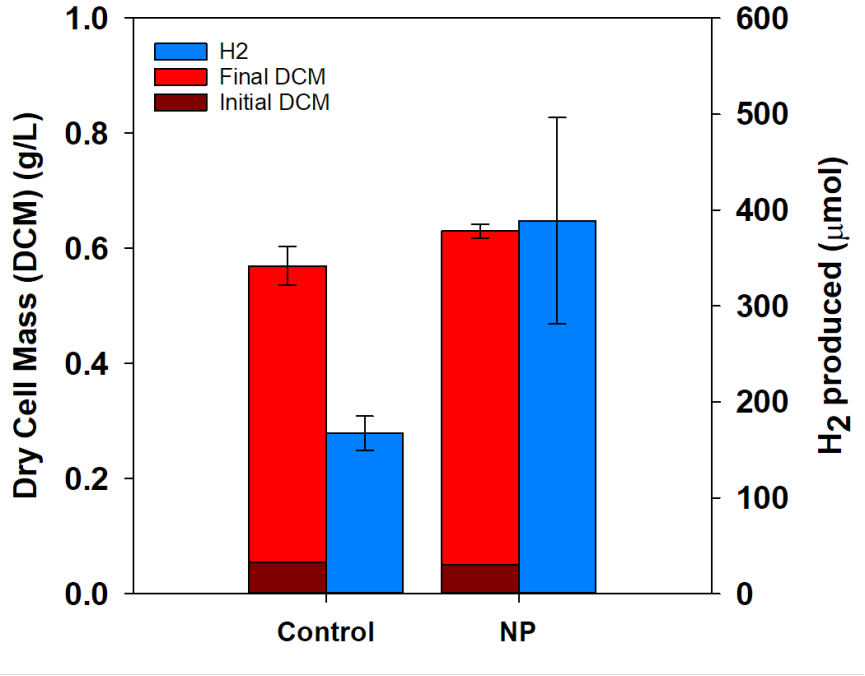

Figure 5.4: Enhancement of Hydrogen Production due to Light Enhancement by Gold-Shell Nanoparticles.

CHAPTER 6. CONCLUSION

Phototrophic hydrogen production from PNSB remains an interesting pathway for converting waste organic acids to clean energy, but low efficiencies in light conversion restrict the utility of the process. Here we have demonstrated the efficacy of NIR illumination for PNSB growth. Switching to NIR illumination compared to widely used tungsten light sources resulted in 3-fold increase in hydrogen production (60 ± 6 to 167±18 μmol H_2 at 130 W/m^2). Further, the addition of plasmonic nanoparticles in solution resulted in an additional 2-fold increase in hydrogen production (167 ±18 to 398±108 μmol H_2). Another key finding of our work established that part of the generated CO_2 is simultaneously utilized by the bacteria resulting in a higher purity hydrogen gas.

Here the use of gold silica core-shell nanoparticles in solution was able to augment light utilization of PNSB in solution, but future efforts to incorporate plasmonically resonant structures into photofermentation systems could utilize immobilization approaches to secure both the nanoparticles and bacteria. The immobilization of bacteria and nanoparticles in close proximity could more effectively exploit near field enhancement around the bacteria.

APPENDICES

APPENDIX 1. MEDIA RECIPES

Table A1.1: Media Recipes. Complex and defined media recipes used for bacterial growth.

Component (g/L)	Complex 1[27]	Complex 2[27]	Complex 3[54]	Defined 1[55]	Defined 2[56]
Sodium Acetate			2.74	5.74	5.74
Sodium Glutamate				1.18	1.18
Tryptic Soy Broth	15				
Yeast Extract		10	0.2		
K_2HPO_4		1			
$MgSO_4$		0.5		0.12	0.24
L-cysteine		0.6			
NH_4Cl			0.65		1
Na_2HPO_4				6.8	6.9
KH_2PO_4				3	3
NaCl				0.58	0.5
$CaCl_2$●2H2O				0.1 mM	0.015
Thiamine HCl				1 mg/L	
Trace Metals Stock				10 mL/L	

Table A1.2: Trace Metals Stock. Used in Defined media 1.

Trace Metals Stock (g/L)	
$CaCl_2$●$2H_2O$	0.729
$FeCl_3$●$6H_2O$	1.666
$MnCl_2$	0.064
$ZnCl_2$	0.170
$CuCl_2$●$2H_2O$	0.043
CoCl●$6H_2O$	0.060
Na_2MoO4●$2H_2O$	0.060

APPENDIX 2. MODIFIED GOMPERTZ FIT MATLAB CODE

```
% import growth data table as growth_data,
% column 1 ~ time (hours) column 2
% column 2 ~ cell density DCM g/L
%growth_data = table2array(growth_data);
%X = growth_data(:,1);
y = growth_data(:,3);

modelfun = @(b,x) b(1)*exp(-exp(((b(2)*exp(1))/b(1))*(b(3)-x)+1));

%modelfun = @(b,x)b(1) + b(2)*x(:,1).^b(3) + ...
%    b(4)*x(:,2).^b(5);
beta0 = [0.24 .0005 20];
mdl = fitnlm(X,y,modelfun,beta0)

b1 = table2array(mdl.Coefficients(1,1));
b2 = table2array(mdl.Coefficients(2,1));
b3 = table2array(mdl.Coefficients(3,1));
X_model = linspace(0,200);
Y_model = b1*exp(-exp(((b2*exp(1))/b1)*(b3-X_model)+1));

plot(X,y,'ro',X_model,Y_model,'k-');
```

REFERENCES

1 Adessi, A. & De Philippis, R. Photobioreactor design and illumination systems for H2 production with anoxygenic photosynthetic bacteria: A review. *International Journal of Hydrogen Energy* **39**, 3127-3141, doi:10.1016/j.ijhydene.2013.12.084 (2014).

2 Larimer, F. W. *et al.* Complete genome sequence of the metabolically versatile photosynthetic bacterium Rhodopseudomonas palustris. *Nature Biotechnology* **22**, 55-61, doi:10.1038/nbt923 (2004).

3 Lo, K.-J., Lin, S.-S., Lu, C.-W., Kuo, C.-H. & Liu, C.-T. Whole-genome sequencing and comparative analysis of two plant-associated strains of Rhodopseudomonas palustris (PS3 and YSC3). *Scientific Reports* **8**, doi:10.1038/s41598-018-31128-8 (2018).

4 McKinlay, J. B. & Harwood, C. S. Photobiological production of hydrogen gas as a biofuel. *Curr Opin Biotechnol* **21**, 244-251, doi:10.1016/j.copbio.2010.02.012 (2010).

5 Hülsen, T. *et al.* White and infrared light continuous photobioreactors for resource recovery from poultry processing wastewater – A comparison. *Water Research* **144**, 665-676, doi:10.1016/j.watres.2018.07.040 (2018).

6 Kawagoshi, Y., Oki, Y., Nakano, I., Fujimoto, A. & Takahashi, H. Biohydrogen production by isolated halotolerant photosynthetic bacteria using long-wavelength light-emitting diode (LW-LED). *International Journal of Hydrogen Energy* **35**, 13365-13369, doi:10.1016/j.ijhydene.2009.11.121 (2010).

7 Liao, Q. *et al.* Formation and hydrogen production of photosynthetic bacterial biofilm under various illumination conditions. *Bioresource Technology* **101**, 5315-5324, doi:10.1016/j.biortech.2010.02.019 (2010).

8 Turon, V., Anxionnaz-Minvielle, Z. & Willison, J. C. Replacing incandescent lamps with an LED panel for hydrogen production by photofermentation: Visible and NIR wavelength requirements. *International Journal of Hydrogen Energy* **43**, 7784-7794, doi:10.1016/j.ijhydene.2018.03.019 (2018).

9 Jain, P. K., Lee, K. S., El-Sayed, I. H. & El-Sayed, M. A. Calculated Absorption and Scattering Properties of Gold Nanoparticles of Different Size, Shape, and Composition: Applications in Biological Imaging and Biomedicine. *The Journal of Physical Chemistry B* **110**, 7238-7248, doi:10.1021/jp057170o (2006).

10 Her, S., Jaffray, D. A. & Allen, C. Gold nanoparticles for applications in cancer radiotherapy: Mechanisms and recent advancements. *Advanced drug delivery reviews* **109**, 84-101 (2017).

11 Amendola, V., Pilot, R., Frasconi, M., Maragò, O. M. & Iatì, M. A. Surface plasmon resonance in gold nanoparticles: a review. *Journal of Physics: Condensed Matter* **29**, 203002, doi:10.1088/1361-648X/aa60f3 (2017).

12 Li, J. T. *et al.* Plasmon-induced resonance energy transfer for solar energy conversion. *Nature Photonics* **9**, 601-+, doi:10.1038/nphoton.2015.142 (2015).

13 Yu, Z. F., Raman, A. & Fan, S. H. Fundamental limit of nanophotonic light trapping in solar cells. *Proceedings of the National Academy of Sciences of the United States of America* **107**, 17491-17496, doi:10.1073/pnas.1008296107 (2010).

14 Oldenburg, S. J., Jackson, J. B., Westcott, S. L. & Halas, N. Infrared extinction properties of gold nanoshells. *Applied Physics Letters* **75**, 2897-2899 (1999).
15 Sakurai, H., Masukawa, H., Kitashima, M. & Inoue, K. Photobiological hydrogen production: Bioenergetics and challenges for its practical application. *Journal of Photochemistry and Photobiology C: Photochemistry Reviews* **17**, 1-25, doi:10.1016/j.jphotochemrev.2013.05.001 (2013).
16 Madigan, M. T. *Brock biology of microorganisms*. 12th ed edn, (Pearson/Benjamin Cummings, 2009).
17 Hallenbeck, P. C. Microbial paths to renewable hydrogen production. *Biofuels* **2**, 285-302, doi:10.4155/bfs.11.6 (2011).
18 McKinlay, J. B. & Harwood, C. S. Photobiological production of hydrogen gas as a biofuel. *Current Opinion in Biotechnology* **21**, 244-251, doi:10.1016/j.copbio.2010.02.012 (2010).
19 Eady, R. R. Structure−Function Relationships of Alternative Nitrogenases. *Chemical Reviews* **96**, 3013-3030, doi:10.1021/cr950057h (1996).
20 Williams, C. R. & Bees, M. A. Mechanistic modeling of sulfur-deprived photosynthesis and hydrogen production in suspensions of *Chlamydomonas reinhardtii*: Modeling of Sulfur-Deprived H2 Production. *Biotechnology and Bioengineering* **111**, 320-335, doi:10.1002/bit.25023 (2014).
21 McKinlay, J. B. *et al.* Non-growing Rhodopseudomonas palustris Increases the Hydrogen Gas Yield from Acetate by Shifting from the Glyoxylate Shunt to the Tricarboxylic Acid Cycle. *Journal of Biological Chemistry* **289**, 1960-1970, doi:10.1074/jbc.M113.527515 (2014).
22 McKinlay, J. B. & Harwood, C. S. Carbon dioxide fixation as a central redox cofactor recycling mechanism in bacteria. *Proceedings of the National Academy of Sciences* **107**, 11669-11675, doi:10.1073/pnas.1006175107 (2010).
23 Luer, L. *et al.* Tracking energy transfer between light harvesting complex 2 and 1 in photosynthetic membranes grown under high and low illumination. *Proceedings of the National Academy of Sciences* **109**, 1473-1478, doi:10.1073/pnas.1113080109 (2012).
24 Cogdell, R. J. *et al.* How Photosynthetic Bacteria Harvest Solar Energy. *J. BACTERIOL.* **181**, 11 (1999).
25 LaSarre, B. *et al.* Restricted Localization of Photosynthetic Intracytoplasmic Membranes (ICMs) in Multiple Genera of Purple Nonsulfur Bacteria. *mBio* **9**, e00780-00718, /mbio/00789/00784/mBio.00780-00718.atom, doi:10.1128/mBio.00780-18 (2018).
26 Zwietering, M. H., Jongenburger, I. & Rombouts, F. M. Modeling of the Bacterial Growth Curve. *APPL. ENVIRON. MICROBIOL.* **56**, 7 (1990).
27 *Rhodopseudomonas palustris (Molisch) van Niel ATCC ® BAA-98™*.
28 Skjånes, K., Andersen, U., Heidorn, T. & Borgvang, S. A. Design and construction of a photobioreactor for hydrogen production, including status in the field. *Journal of Applied Phycology* **28**, 2205-2223, doi:10.1007/s10811-016-0789-4 (2016).
29 Hübert, T., Boon-Brett, L., Black, G. & Banach, U. Hydrogen sensors – A review. *Sensors and Actuators B: Chemical* **157**, 329-352, doi:10.1016/j.snb.2011.04.070 (2011).

30 *EC4-1000-H2, Gas Sensor - Electrochemical, SGX Sensortech Limited (formerly e2v)*.
31 Catchpole, K. a. & Polman, A. Plasmonic solar cells. *Optics express* **16**, 21793-21800 (2008).
32 Chen, C.-D., Cheng, S.-F., Chau, L.-K. & Wang, C. C. Sensing capability of the localized surface plasmon resonance of gold nanorods. *Biosensors Bioelectronics* **22**, 926-932 (2007).
33 Ghasemi, S., Hashemian, S., Alamolhoda, A., Gocheva, I. & Setayesh, S. R. Plasmon enhanced photocatalytic activity of Au@ TiO2-graphene nanocomposite under visible light for degradation of pollutants. *Materials Research Bulletin* **87**, 40-47 (2017).
34 Ghosh, P., Han, G., De, M., Kim, C. K. & Rotello, V. M. Gold nanoparticles in delivery applications. *Advanced drug delivery reviews* **60**, 1307-1315 (2008).
35 Lee, K.-S. & El-Sayed, M. A. Gold and silver nanoparticles in sensing and imaging: sensitivity of plasmon response to size, shape, and metal composition. *The Journal of Physical Chemistry B* **110**, 19220-19225 (2006).
36 Li, Y., Wang, H., Feng, Q., Zhou, G. & Wang, Z.-S. Gold nanoparticles inlaid TiO 2 photoanodes: a superior candidate for high-efficiency dye-sensitized solar cells. *Energy Environmental Science* **6**, 2156-2165 (2013).
37 Lu, D. *et al.* Highly efficient visible-light-induced photoactivity of Z-scheme g-C3N4/Ag/MoS2 ternary photocatalysts for organic pollutant degradation and production of hydrogen. *ACS Sustainable Chemistry Engineering* **5**, 1436-1445 (2017).
38 Sahoo, S. K., Misra, R. & Parveen, S. in *Nanomedicine in Cancer* 73-124 (Pan Stanford, 2017).
39 Wang, C. C. *et al.* Optical and electrical effects of gold nanoparticles in the active layer of polymer solar cells. *Journal of Materials Chemistry* **22**, 1206-1211 (2012).
40 Wu, J.-L. *et al.* Surface plasmonic effects of metallic nanoparticles on the performance of polymer bulk heterojunction solar cells. *ACS nano* **5**, 959-967 (2011).
41 Loo, C. *et al.* Nanoshell-enabled photonics-based imaging and therapy of cancer. *Technology in cancer research treatment* **3**, 33-40 (2004).
42 Petryayeva, E. & Krull, U. J. Localized surface plasmon resonance: nanostructures, bioassays and biosensing—a review. *Analytica chimica acta* **706**, 8-24 (2011).
43 Mie, G. Contributions to the optics of turbid media, particularly of colloidal metal solutions. *Ann. Phys.* **25**, 377-445 (1908).
44 Nehru, N. *et al.* Differentiating surface and bulk interactions using localized surface plasmon resonances of gold nanorods. *Optics express* **20**, 6905-6914 (2012).
45 Nehru, N., Linliang, Y., Yinan, W. & Hastings, J. T. Using U-shaped localized surface plasmon resonance sensors to compensate for nonspecific interactions. *IEEE Trans. Nanotechnology* **13**, 55-61 (2014).
46 Shakiba, A. *et al.* Silver-free gold nanocages with near-infrared extinctions. *ACS Omega* **1**, 456-463 (2016).
47 Chan, G. H., Zhao, J., Hicks, E. M., Schatz, G. C. & Van Duyne, R. P. Plasmonic properties of copper nanoparticles fabricated by nanosphere lithography. *Nano Letters* **7**, 1947-1952 (2007).

48 Grayson, K. J. *et al.* Augmenting light coverage for photosynthesis through YFP-enhanced charge separation at the Rhodobacter sphaeroides reaction centre. *Nature Communications* **8**, 13972, doi:10.1038/ncomms13972 (2017).

49 Lishchuk, A. *et al.* Turning the challenge of quantum biology on its head: biological control of quantum optical systems. *Faraday Discussions*, 10.1039.C1038FD00241J, doi:10.1039/C8FD00241J (2019).

50 Lishchuk, A. *et al.* A synthetic biological quantum optical system. *Nanoscale* **10**, 13064-13073, doi:10.1039/C8NR02144A (2018).

51 Tsargorodska, A. *et al.* Strong Coupling of Localized Surface Plasmons to Excitons in Light-Harvesting Complexes. *Nano Letters* **16**, 6850-6856, doi:10.1021/acs.nanolett.6b02661 (2016).

52 Abadeer, N. S. & Murphy, C. J. Recent Progress in Cancer Thermal Therapy Using Gold Nanoparticles. *The Journal of Physical Chemistry C* **120**, 4691-4716, doi:10.1021/acs.jpcc.5b11232 (2016).

53 Lee, Y. V. & Tian, B. Learning from Solar Energy Conversion: Biointerfaces for Artificial Photosynthesis and Biological Modulation. *Nano Lett* **19**, 2189-2197, doi:10.1021/acs.nanolett.9b00388 (2019).

54 Carlozzi, P. & Sacchi, A. Biomass production and studies on Rhodopseudomonas palustris grown in an outdoor, temperature controlled, underwater tubular photobioreactor. *Journal of Biotechnology* **88**, 239-249, doi:10.1016/S0168-1656(01)00280-2 (2001).

55 Zhao, J., Baba, T., Mori, H. & Shimizu, K. Effect of zwf gene knockout on the metabolism of Escherichia coli grown on glucose or acetate. *Metabolic Engineering* **6**, 164-174, doi:10.1016/j.ymben.2004.02.004 (2004).

56 Liao, Y.-C. *et al.* An Experimentally Validated Genome-Scale Metabolic Reconstruction of Klebsiella pneumoniae MGH 78578, iYL1228. *Journal of Bacteriology* **193**, 1710-1717, doi:10.1128/JB.01218-10 (2011).

VITA

John Craven graduated Magna Cum Laude with a B.S. in Chemistry and Mathematics from the University of Kentucky in 2013. In 2016 he began his Master's work at the University of Kentucky Department of Chemical Engineering.

Professional Positions

ASRC Rubber Company (Michelin Group). Quality Control Chemist. 2013-2014

Presentations

John Craven, R. Sarma, M. Sultan, T. Hastings, D.Y. Kim, D. Bhattacharyya, **Near-IR Surface Plasmon enhanced Conversion of Organic Acids to H_2 Using Phototrophic Bacteria.** KY NSF EPSCoR Super Collider Graduate Student Conference, Lexington, Ky, April 2019.

Publications

Andrew Colburn, RJ Vogler, Mariah Bezold, *John Craven*, Dibakar Bhattacharyya **Composite Membranes Derived from Cellulose and Lignin Sulfonate for Selective Separations and Antifouling Aspects.** *Nanomaterials* 2019, 9(6), 867; https://doi.org/10.3390/nano9060867

John Craven, M. Sultan, R. Sarma, S. Wilson, N. Meeks, D.Y. Kim, T. Hastings, D. Bhattacharyya, **Near-IR Surface Plasmon Enhanced Conversion of Organic Acids to Hydrogen Using Phototrophic Bacteria.** *PNAS* 2019, *To be submitted*